*Progress In Electromagnetics Research Letters, Vol. 106, 41–47, 2022*

# A Compact Patch Antenna with a Fractal Structure for Beidou (COMPASS) Navigation System

**Encheng Wang[1], Mengxin Liu[1, *], Daming Lin[2], and Jie Wang[1]**

**Abstract**—A circularly polarized (CP) patch antenna with a fractal structure that can be applied to the BeiDou navigation satellite system (BDS) is proposed. Etching two incomplete rings of different sizes with the antenna center as the center on the radiation patch generates CP. By adding a periodic structure based on the Sierpinski Carpet fractal around it, the size can be reduced while the gain is further improved. The dimension of the antenna is $0.35\lambda_o \times 0.35\lambda_o \times 0.03\lambda_o$. Measured results manifest that the impedance bandwidth ($S_{11} < -10\,\text{dB}$) is wider than 40 MHz at 1.561 GHz; the gain in 3-dB axial ratio (AR) bandwidth can reach 3.33 dBi; the beamwidth exceeds 140° in the 3-dB AR bandwidth.

## 1. INTRODUCTION

Beidou navigation satellite system (BDS) is developing rapidly and is widely used in various fields, which can not only transmit location information but also support short message communication [1]. So far, many CP antennas used in global navigation satellite system (GNSS) have been reported [2–6]. Among them, patch antenna can achieve a compact size while generating CP, which is suitable for portable terminals. A hemispherical dielectric resonator antenna with a photonic band-gap (PBG) structure is proposed in [7], which can improve the antenna performance, but antenna size is not miniaturized. An array antenna with a fractal structure can be miniaturized, but its feed network is complex, and its working frequency cannot meet the requirements [8]. Some BDS antennas have also been reported, striving for miniaturization, wide bandwidth, and high gain [9–11]. [9] proposes a miniaturized CP microstrip antenna, but its complex structure is not easy to manufacture. A three-layer antenna is mentioned in [10], using asymmetric ring slot to produce CP, but the cost is high. A patch antenna with a circular slot and a single feed is proposed in [11], which is enlightening.

In this letter, a compact CP patch antenna is proposed, which is miniaturized. Two concentric annular slots with notches and second-order hexagonal groove structures with circumferential periods support the antenna to generate CP radiation without introducing a complex feed network and other disturbances, which can work in the B1 band of BD2 ($1561.098 \pm 2.046$ MHz). A coaxial probe feed is used to generate right-handed circular polarization (RHCP). The proposed antenna is simulated by simulation software Ansoft HFSS, and the simulation and measurement results are compared and discussed.

## 2. ANTENNA DESIGN

Figure 1(a) shows the antenna appearance, and details of the hexagonal groove structure are displayed in Fig. 1(b). $L$ is the length of the antenna. The FR4 substrate thickness is $H$, dielectric coefficient $\varepsilon = 4.4$, and the loss tangent 0.02. The coaxial feed position is set in the center of the antenna to excite

*Received 20 June 2022, Accepted 4 August 2022, Scheduled 25 August 2022*

* Corresponding author: Mengxin Liu (503917501@qq.com).

[1] Information Engineering College, North China University of Technology, Beijing 100144, China. [2] Institute of Highway, Ministry of Transport, Beijing 100088, China.

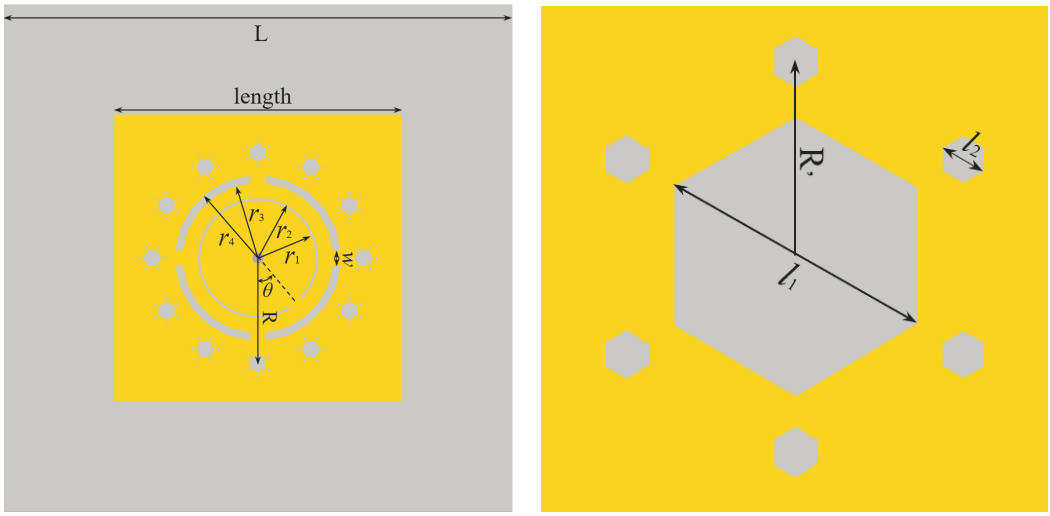


(a) (b)

**Figure 1.** Antenna style. (a) Top side. (b) Second-iteration hexagonal groove fractal structure.

the CP, which can make the antenna have good symmetry. Two annular slots with notches centered at the feed point are used to excite CP, in which the inner radii are $r_1$ and $r_3$, and the outer radii are $r_2$ and $r_4$, respectively. The notch of the inner ring is set at the offset angle $\theta = 50°$, and the outer ring has four notches with a phase difference of 90° to achieve the best impedance matching and RHCP. The width of the notches is $w$. Based on the idea of Sierpinski Carpet fractal, the second-iteration fractal shapes are circumferentially arranged with the feed point as the center and R as the radius, and each unit is periodically arranged at the same angle. Six smaller hexagonal grooves are distributed around each larger hexagonal groove. The distance between the smaller hexagon and larger hexagons is $R'$; the diameter of the larger hexagon is $l_1$; and the diameter of the smaller hexagon is $l_2$. This structure further improves the CP effect of the antenna, reduces the antenna size, and increases the antenna gain.

### 2.1. Number of Hexagonal Grooves

Divide the circumference into different angles corresponding to different numbers of hexagonal grooves. Because the change of the number of hexagonal grooves will affect the effect of the antenna, the side length of the ground plate also needs to be changed to ensure the best CP effect. Table 1 lists the simulated AR and gain results with different numbers of grooves.

**Table 1.** Comparison of results under different number of grooves.

| Number of grooves | Axial Ratio (dB) | Gain (dBi) | $L$ (mm) |
|---|---|---|---|
| 0 | 3.4383 | 3.6188 | 80 |
| 6 | 1.917 | 2.9697 | 76 |
| 12 | 1.6822 | 3.0471 | 73 |
| 18 | 2.1527 | 3.709 | 72 |
| 24 | 3.03 | 3.8872 | 72 |
| 30 | 1.9267 | 3.4698 | 71 |
| 36 | 2.8668 | 3.8431 | 71 |

After comparison, the AR at the center frequency is below 2 dB in both cases of 12 grooves structure and 30 grooves structure with the gain higher than 3 dBi. The gain of the 30 grooves structure is higher, but at this time the radiating patch is almost in saturation, which is the best effect that the 30 grooves

structure can achieve. So, it is decided that the 12 grooves structure is to be the basis, which has the best CP effect but low gain. The small hexagon is etched around it to improve its gain.

### 2.2. Second-Iteration Hexagonal Groove Fractal Structure

Due to the complexity of manufacturing, the second-iteration hexagonal groove fractal structure was chosen. The effect compared with the first-order structure is displayed in Fig. 2. The AR of the second-order structure is lower, and the gain is higher, which is due to its space-filling expanding the equivalent current route of the antenna and further reducing the size of the antenna [12].

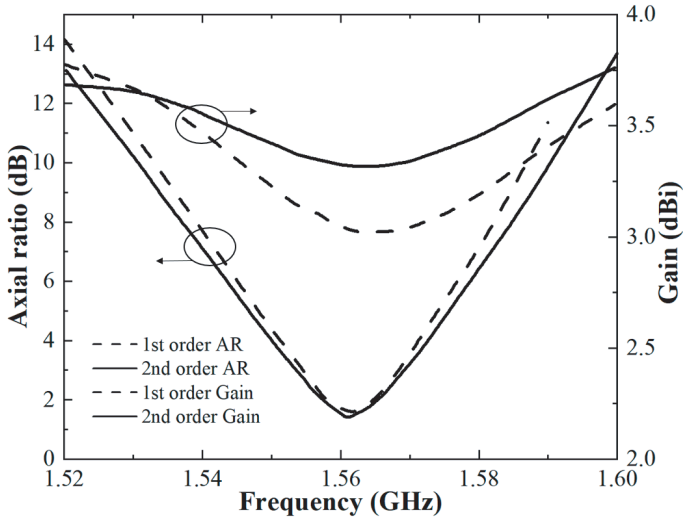


**Figure 2.** Comparison of antenna effects of different orders.

## 3. PARAMETRIC STUDIES

### 3.1. Distance of First-Iteration Fractal Shape, $R$

With other parameters unchanged, the distance $R$ of the center of the first-iteration hexagonal groove fractal shape from the center of the antenna increased from 13.8 mm to 14.2 mm. The AR results are displayed in Fig. 3(a). With the increase of $R$ from 13.8 mm to 14 mm, the antenna operating frequency increases, and the best AR is achieved at 14 mm. In the process of increasing from 14 mm to 14.2 mm, the operating frequency decreases greatly, and the AR becomes more than 3 dB.

### 3.2. Distance of Second-Iteration Fractal Shape, $R'$

With other parameters unchanged, the distance $R'$ of the center of the second-iteration hexagonal groove fractal shape from the center of the first-iteration hexagonal groove fractal shape changed from 1.5 mm to 1.8 mm. Fig. 3(b) shows the AR results. When $R'$ increases from 1.5 mm to 1.7 mm, the operating frequency of the antenna changes to 1.561 GHz, and the AR becomes the best. When $R'$ is further increased to 1.8 mm, the operating frequency changes slightly, but the AR becomes worse.

### 3.3. Diameter of First-Iteration Hexagonal Groove, $l_1$

With other parameters unchanged, the diameter of the first-iteration hexagonal groove changed from 1.6 mm to 2.8 mm, and the AR result is shown in Fig. 3(c). When $l_1$ is changed from 1.6 mm to 2.0 mm, the operating frequency of the antenna becomes about 1.561 GHz, but the effect of the AR becomes worse. When it is further increased to 2.4 mm, the AR decreases greatly under the condition that the operating frequency does not change much, which shows that the antenna changes from linear

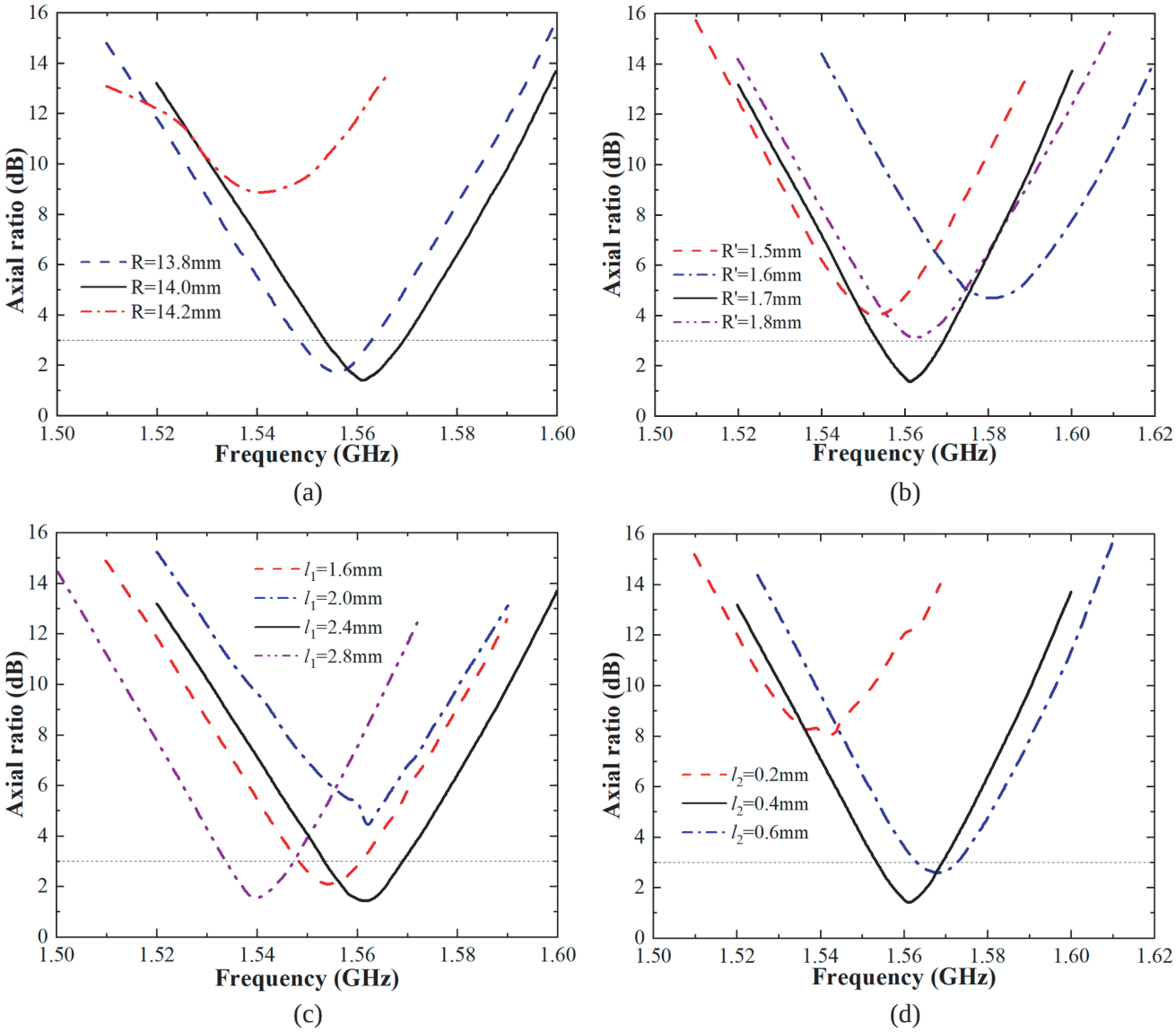


**Figure 3.** AR results under different parameters. (a) $R$. (b) $R'$. (c) $l_1$. (d) $l_2$.

polarization to circular polarization. When it changes from 2.4 mm to 2.8 mm, the operating frequency drops, which does not meet the frequency band requirements. Therefore, $l_1$ is finally determined to be 2.4 mm.

### 3.4. Diameter of Second-Iteration Hexagon Groove, $l_2$

With other parameters unchanged, the diameter of the second-iteration hexagonal groove changed from 0.2 mm to 0.6 mm. Fig. 3(d) displayed the AR result. As $l_2$ gets longer, the operation frequency of the antenna increases. Finally, the diameter of the second-iteration hexagonal groove is determined according to the best simulation result when $l_2 = 0.4$ mm.

### 3.5. Dimensions of Ground Plate and Substrate

Generally, as the ground size increases, the gain of the antenna becomes higher, and as the substrate thickness increases, the operating frequency of the antenna decreases [13]. The following formula is used

to estimate the antenna size:

$$L = 300/\left(2 \times f \times \sqrt{\varepsilon_r}\right) \text{ (mm)} \quad (1)$$

$L$ is the side length of the ground plane, $f$ the working frequency, and $\varepsilon_r$ the relative permittivity of the substrate. The antenna side length is calculated to be 45.8 mm [14]. Besides the gain, the size of the substrate will also affect the effect of CP. Adjust the parameter on the basis of antenna structure and the requirements of operating frequency and performance, and finally determine the antenna size 67.3 mm × 67.3 mm. Although increasing the thickness of the substrate will increase the bandwidth, an excessively thick substrate will not only destroy the low profile of the antenna but also affect the radiation efficiency of the antenna. Considering the performance of the antenna, the dielectric constant, and the loss of the dielectric substrate, and adjusting the thickness according to the CP effect obtained by simulation, the thickness of the substrate is determined to be 4.8 mm.

## 4. RESULTS AND DISCUSSION

Table 2 lists the parameters of the proposed antenna working at 1.561 GHz. The fabricated antenna is plotted in Fig. 4. The results comparisons of $S_{11}$ and gain are depicted in Fig. 5(a). The impedance bandwidth less than −10 dB is greater than 40 MHz, and the measured gain at the center frequency is about 3.3 dBi. Fig. 5(b) reveals the radiation patterns of simulated and measured results at 1.561 GHz. The RHCP effect is proved to be good. Although the operating methods and actual losses in the manufacturing and measuring process may cause some slight differences between the results, the measurement results are generally similar to the simulation results. Table 3 compares the characteristics of several antennas of the same type. The proposed antenna is more compact and has better performance.

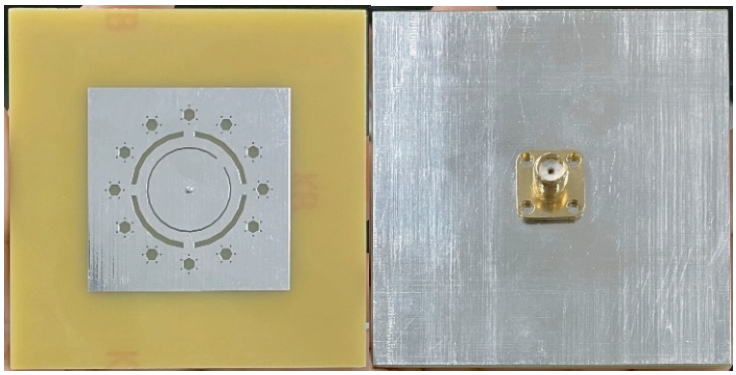

(a)

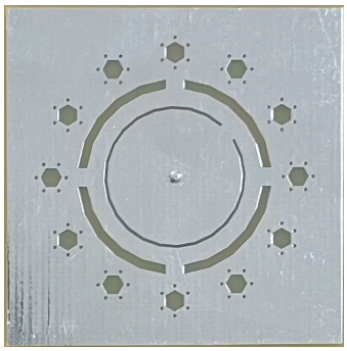

(b)

**Figure 4.** Fabricated antenna. (a) Overall appearance. (b) Radiation patch.

**Table 2.** Optimal parameters of antennas.

| Parameter | $L$ | $H$ | length | $w$ |
|---|---|---|---|---|
| Value (mm) | 67.3 | 4.8 | 38.1 | 2.1 |
| Parameter | $R$ | $R'$ | $l_1$ | $l_2$ |
| Value (mm) | 14.0 | 1.7 | 2.4 | 0.4 |
| Parameter | $r_1$ | $r_2$ | $r_3$ | $r_4$ |
| Value (mm) | 0.3 | 0.22 | 1.27 | 0.4 |

**Table 3.** Comparison between the proposed antenna and similar cases.

| Reference | Size (mm) | Freq. (GHz) | $S_{11}$ (dB) | Gain (dBi) | Substrate material |
|---|---|---|---|---|---|
| 3 | $70 \times 70 \times 26$ | 1.561 | $-23$ | 3.3 | FR-4 |
| 4 | $60 \times 60 \times 18$ | 1.575 | $-25$ | 3 | F4bm-2 |
| 12 | $80 \times 80 \times 4.8$ | 1.561 | $-24$ | 3 | FR-4 |
| Proposed | $67.3 \times 67.3 \times 4.8$ | 1.561 | $-27$ | 3.3 | FR-4 |

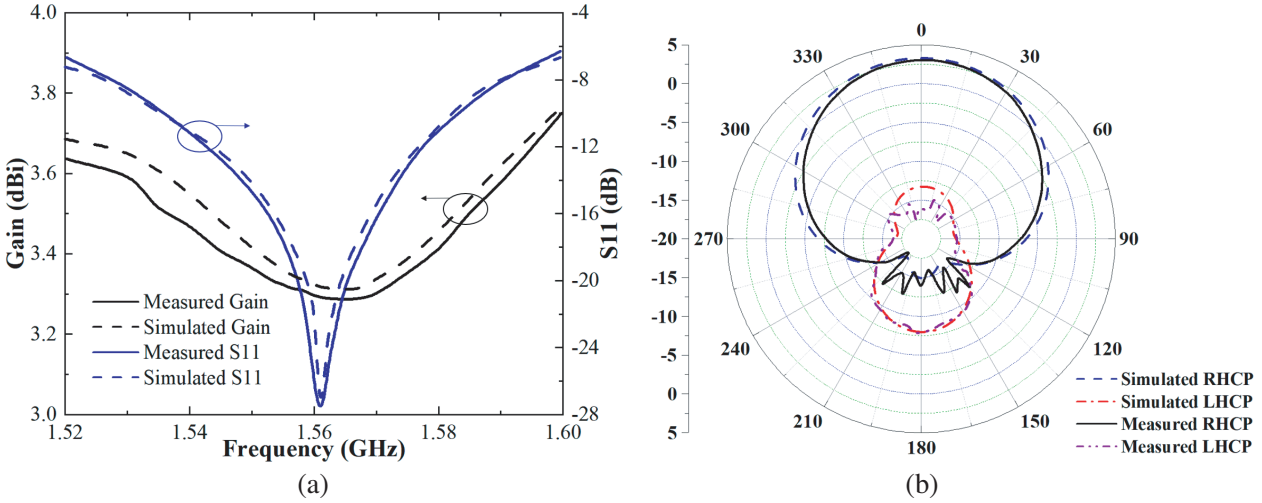


**Figure 5.** Simulation and measuring results. (a) Gain and $S_{11}$. (b) Radiation patterns at 1.561 GHz.

## 5. CONCLUSION

In order to meet the needs of BDS, a compact single-feed patch antenna is proposed. Circular polarization is generated by using two annular slots with notches. A second-iteration hexagonal groove fractal structure is proposed, which can significantly decrease the antenna dimension and improve its performance. The feasibility of the antenna scheme is verified by simulation and measurement. The experimental results testify that compared with the antenna without fractal structure (number of grooves is 0), the size of the proposed antenna is reduced by about 29% (comparison of volume). The introduction of the hexagonal groove fractal structure can increase the current length on the surface of the radiation patch, which can make up for the gain reduction caused by the antenna size reduction. The high symmetry of the fractal structure also ensures the CP effect of the antenna. Therefore, using the fractal structure can effectively reduce the antenna size while maintaining good antenna performance. The fabricated antenna performs well at 1.561 GHz, meets the needs of the BDS B1 band, achieves miniaturization, medium gain, low cost, and enough beamwidth, which has a great value for the research of antenna applied in BDS.

## ACKNOWLEDGMENT

The authors are grateful to the Project of Young YuYou of North China University of Technology, 2018 and the Research on Key Technologies of accurate positioning of BINGTUAN transportation key vehicles and infrastructure based on Beidou under Grant 2108AB028.

## REFERENCES

1. Xiao, B., H. Wong, M. Li, B. Wang, and K. L. Yeung, "Dipole antenna with both odd and even modes excited and tuned," *IEEE Trans. Antennas Propag.*, Vol. 70, No. 3, 1643–1652, 2022.
2. Musthafa, A. M., M. Khalily, A. Araghi, O. Yurduseven, and R. Tafazolli, "Compact multimode quadrifilar helical antenna for GNSS-R applications," *IEEE Antennas and Wireless Propag. Lett.*, Vol. 21, No. 4, 755–759, 2022.
3. Zhang, H., Y. Guo, and G. Wang, "A wideband circularly polarized crossed-slot antenna with stable phase center," *IEEE Antennas and Wireless Propag. Lett.*, Vol. 18, No. 5, 941–945, 2019.
4. Sun, C., Z. Wu, and B. Bai, "A novel compact wideband patch antenna for GNSS application," *IEEE Trans. Antennas Propag.*, Vol. 65, No. 12, 7334–7339, 2017.
5. Choudhary, S. D., A. Srivastava, and M. Kumar, "Design of single-fed dual-polarized dual-band slotted patch antenna for GPS and SDARS applications," *Microw. Opt. Technol. Lett.*, 1–8, 2020.
6. Guo, L., P. Zhang, F. Zeng, Z. Zhang, and C. Zhang, "A novel four-arm planar spiral antenna for GNSS application," *IEEE Access*, Vol. 9, 168899–168906, 2021.
7. Gupta, S., P. Kshirsagar, and B. Mukherjee, "Sierpinski fractal inspired inverted pyramidal DRA for wide band applications," *Electromagnetics*, Vol. 38, No. 2, 103–112, 2018.
8. Kuzu, S. and N. Akcam, "Array antenna using defected ground structure shaped with fractal form generated by apollonius circle," *IEEE Antennas Wireless Propag. Lett.*, Vol. 16, 1020–1023, 2017.
9. Sun, C., H. Zheng, L. Zhang, et al., "A compact frequency-reconfigurable patch antenna for Beidou (COMPASS) navigation system," *IEEE Antennas Wireless Propag. Lett.*, Vol. 13, 967–970, 2014.
10. Liu, Z., S. Fang, S. Zhu, et al., "BeiDou navigation terminal multi-mode asymmetric slots circularly polarized microstrip antenna," *Proceedings of 2014 3rd Asia-Pacific Conference on Antennas and Propagation*, 382–385, Harbin, China, Jul. 26–29, 2014.
11. Zheng, K. and Q. Chu, "A novel annular slotted center-fed BeiDou antenna with a stable phase center," *IEEE Antennas Wireless Propag. Lett.*, Vol. 17, No. 3, 364–367, 2018.
12. Zheng, K. and Q. Chu, "A small symmetric-slit-shaped and annular slotted BeiDou antenna with stable phase center," *IEEE Antennas Wireless Propag. Lett.*, Vol. 17, No. 1, 146–149, 2018.
13. Nasimuddin, X. Qing, and Z. N. Chen, "A compact circularly polarized slotted patch antenna for GNSS applications," *IEEE Trans. Antennas Propag.*, Vol. 62, No. 12, 6506–6509, 2014.
14. Wang, L., X.-X. Yang, T. Lou, and S. Gao, "A miniaturized differentially fed patch antenna based on capacitive slots," *IEEE Antennas Wireless Propag. Lett.*, Vol. 21, No. 7, 1472–1476, 2022.